Offline tool trajectory compensation for cutting forces induced errors in a portable machine tool

Checchi, Alessandro; Dalla Costa, Giuseppe; Merrild, Christian Haastrup; Bissacco, Giuliano; Hansen, Hans Nørgaard

Published in:
Procedia CIRP

Link to article, DOI:
10.1016/j.procir.2019.05.025

Publication date:
2019

Document Version
Publisher's PDF, also known as Version of record

Available online at www.sciencedirect.com

ScienceDirect

Procedia CIRP 82 (2019) 527–531

www.elsevier.com/locate/procedia

17th CIRP Conference on Modelling of Machining Operations

Offline tool trajectory compensation for cutting forces induced errors in a portable machine tool

Alessandro Checchi[a]*, Giuseppe Dalla Costa[a], Christian Haastrup Merrild[b], Giuliano Bissacco[a], Hans Nørgaard Hansen[a]

[a]*Technical University of Denmark DTU, Department of Mechanical Engineering, Produktionstorvet Building: 427, 2800 Kgs. Lyngby 2800, Denmark*
[b]*Danish Advanced Manufacturing Research Center, DAMRC, Sandagervej 10, Herning 7400, Denmark*
* Corresponding author. Tel.: +45 45254834; *E-mail address:* aleche@mek.dtu.dk

Abstract

Portable machine tools are designed to reduce costs and resources necessary to perform dedicated tasks, such as milling of large components like wind turbine hubs. Such machines however lack in performance (e.g. stiffness, accuracy, thermal stability) with respect to conventional machine tools and may require compensation strategies to guarantee adequate accuracy. An offline compensation methodology, involving tool trajectory modification, based on the calculation of tool center point displacements from prediction of cutting forces and static stiffness characterization was implemented on a portable machine tool. The offline compensation was validated through a posteriori comparison with the nominal cutting conditions.

Peer-review under responsibility of the scientific committee of The 17th CIRP Conference on Modelling of Machining Operations

Keywords: Milling; Deformation; Compensation

1. Introduction

Production and maintenance costs of wind turbines represents the majority of the costs for a wind power plant [1], Together with the increase of turbine efficiency, the reduction of these costs represents an hot topic in research nowadays. Regarding the production of wind turbine hubs, the introduction of portable dedicated machine tools can reduce the costs of production and logistics as well as the manufacturing downtime [2, 3]. In this context a portable machine tool has been developed for machining of wind turbine hubs. The hub consists of a large cast iron component with circular flanges connecting the rotor blades and the main shaft. The main required machining operations of the cast part, to consider in the design of the machine tool, are face milling and drilling [4].The portable machine tool follows the design principle of "small machine in large workpieces" [5]. It consists of a fixed frame mounted directly on the hub which connects the moving axes and the spindle in a direct coupling fashion [2]. To account for the axial symmetry of the flanges to be machined, the moving axes consist of a rotary axis (c) which carries two linear axes, see Fig.1, generating a cylindrical coordinate system and

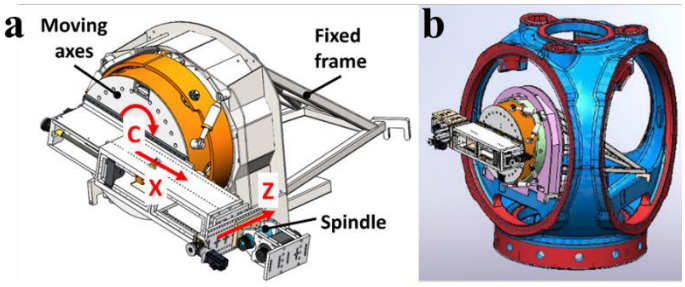

Fig. 1. (a) Drawing of the machine and its supporting frame, indicated also the moving axis. (b) View of the machine mounted on the hub in a typical working condition.

2212-8271
Peer-review under responsibility of the scientific committee of The 17th CIRP Conference on Modelling of Machining Operations
10.1016/j.procir.2019.05.025

a cylindrical working volume. Portable machines built for a dedicated task such as the one presented in this paper obey to precise specifications regarding volume and weight, to satisfy the requirements of portability and flexibility. The principal drawback concerns the general loss in the volume production capability of the machine, mostly related to a loss in the mechanical stiffness characteristics. Problems regarding not only the machine efficiency optimization but also the fulfilment of tolerance requirements may arise from diminished structural rigidity. In this context, cutting forces induced errors on the machined part can be of significant impact on the cost balance and achievement of tolerance requirements.

1.1. Tool-path compensation modelling

Different strategies have been developed to address the cutting forces induced errors, one of these approaches is the offline tool path compensation [6,9-11]. This technique was proved a valuable tool to reduce surface errors generated by machine tool deflection. In this approach, the tool path is changed based on the prediction of the machine tool deflection and relative surface generation error. In the present paper, the offline tool path compensation is based on a cutting force model, a semi-empirical model developed from Armarego's theories [6], and a machine tool deflection model, based on a characterization of the machine stiffness [6, 9].

For predicting cutting forces for the spheroidal cast iron, which wind turbine hubs are made of, a mechanistic cutting force model [7] was employed. It is based on the discretization of a generic cutting edge into infinitesimal linear segments, each of those considered as an oblique cutting operation [6]. The force on each segments can be described as in Eq. (1):

$$dF = K_{i_c} * dA + K_{i_e} * db \qquad (1)$$

Where dA is the discretized chip thickness area, engaged by each infinitesimal cutting edge, db is the discretized chip width and K_{ic} and K_{ie} are respectively the specific cutting force coefficients and the edge force coefficients. In previous studies a mechanistic modelling approach was proved reliable to predict cutting forces for materials prone to chip fragmentation such as spheroidal cast iron [7]; therefore, validation of this model is not treated in depth in the present paper.

The cutting-force induced errors are calculated by assuming the cantilever beam approximation used in combination with the machine-tool stiffness characterization, a schematic representation of the model is given in Figure 2. It is assumed that the cutting force is acting as a concentrated force at the middle point of the axial depth of cut [10]. Variations of the cutting force with the angular position along the tool axis are neglected because the axial depth of cut was relatively small for the tested cases. Hence, the deflection is calculated as follow, eq. (2):

$$d = \frac{F}{E*I}\left(\frac{L*z^2}{2} - \frac{z^3}{6}\right) + \frac{F}{K} \qquad (2)$$

With d the total machine deflection, F the cutting force, K the machine-tool stiffness experimentally measured, E the Young's modulus of the tool material, I the tool inertia momentum, L the length of the tool and z the coordinate at which the cutting force is applied.

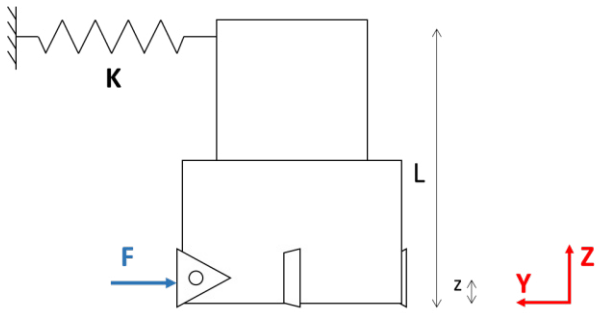

Fig. 2. Schematic representation of the model used to described the machine-tool stiffness and to calculate the overall deflection due to the cutting forces.

The tool path correction is then iteratively calculated, as defined by Cho and Seo [9], setting the desired tolerance at 10 µm. Iteration is necessary as the cutting forces are also dependent on the effective tool engagement and in turn on the machine-tool deflection.

A characterization of the machine stiffness is carried out experimentally in the machine working volume with the intent of realizing a stiffness map. A more detailed description of the procedure is found in the next section.

Tests of linear path machining were conducted to validate the deflection predictions, using the machine in real working conditions, i.e. mounted on the hub. In the same configuration, similar linear path milling tests were also conducted to validate the offline tool path compensation approach.

2. Material and methods

2.1. Procedure to measure the machine stiffness

The experimental stiffness characterization of the machine was conducted in conditions as similar as possible to the working conditions, that is, the machine was mounted on the hub in order to machine the blade flange, Figure 1. In this configuration, the hub structure and in particular the hub-machine connections may have a role in the overall deflection, therefore to take into account this contribution, a fixture was designed to apply the same force to the hub and the machine. The fixture is shown in Figure 3 and it consists of a dynamometer, a cylindrical housing bolted on it and a tool-holder-shaped third part that is attached to the machine's spindle. The housing radius and height are larger than the tool holder to allow free movement of the latter inside the housing.

The fixture as it is described was bolted on five different regions of the hub blade flange, see Figure 4, and in each of these the system stiffness was measured along the three principal directions, radial (along the X axis), circumferential (along the C axis), and axial (along the Z axis). The force was applied by realizing contact between the tool-holder and the housing and then applying a known displacement to the tool center point.

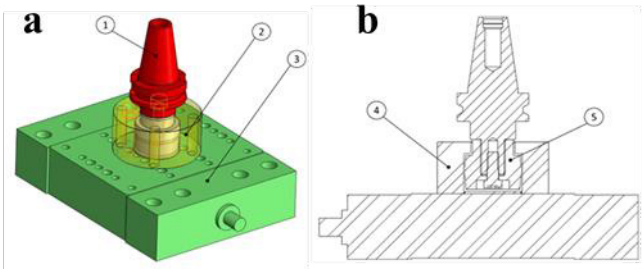

Fig. 3. (a) 3D model of the fixture system, component 1 is the tool-holder, component 2 is the cylindrical housing and component 3 is the dynamometer. (b) Section view, component 4 is the housing, component 5 is the tool-holder-shaped part.

The dynamometer registered the applied force while an inductive displacement sensor measured the effective displacement of the tool-holder, the latter was used for the stiffness calculation. The stiffness measurements were conducted using at least six different values of contact force, varying from 50 N to 2000 N, for each axis and for each direction.

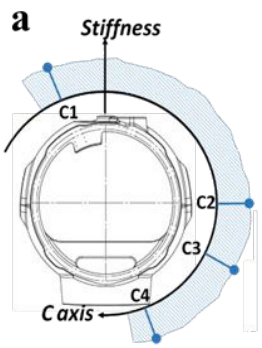

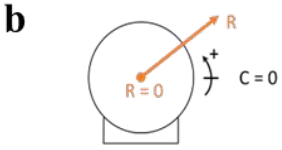

	Coordinates in the machine Polar Reference System	
Position	C angular coordinate [°]	R radial coordinate [mm]
C1	115	1507
C1.2	115	1347
C2	0	1569
C3	-30	1569
C4	-70	1569

Fig. 4. (a) Schematic representation of the stiffness map as function of the machine position on the C-axis. The indicated positions, C1-C4 are the positions were the stiffness characterization was carried out. (b) Reference system convention used during the stiffness testing and the coordinates of each test positions.

2.2. Machining Tests

To validate the deflection model and the offline tool-path compensation, machining tests on small workpieces were carried out. Two separate sets of machining tests were performed, the first one aims at validating the model deflection prediction, and consequently the machine stiffness characterization, while the second one aims at a verification of the offline tool-path compensation performance. Cutting parameters used in the machining tests to validate the deflection prediction, first set of tests as described before, are shown in Table 1. A full factorial approach was used with three repetitions for each test. Cutting speed was constant at 200 m/min. Another set of machining tests were performed applying the calculated compensated trajectory, accordingly to the strategy described above. For these second tests, only one set of cutting parameters was used: Ae = 32 mm, Ap = 1.75 mm, f = 0.1 mm/tooth and cutting speed V = 300 m/min. Three repetitions of the offline compensation tests were carried out. Also, for comparison, a single machining test, with the same cutting parameters, was conducted without applying the trajectory correction.

Table 1. Cutting parameters used in the machining tests.

Parameters	Value
Ae [mm]	16, 40
Ap [mm]	3
Feed rate [mm/tooth]	0.04, 0.08, 0.12

The machining setup, composed by workpieces, dynamometer and connecting plates was fixed on the hub in a convenient location, similarly to the stiffness measurement configuration. The test position on the hub was the C2 in Figure 4. Linear path climb milling operations were performed on workpieces made of the same material of the hub (GJS 400 18U LT spheroidal ductile cast iron). Dimensional measurements of the machined workpieces were performed with a Zeiss Prismo CMM. For this purpose, the machined surfaces were probed along parallel profiles at several positions along the height direction (tool axis direction). The difference between measured and nominal dimensions gives an estimation of the actual trajectory and the deflection of the tool during cutting. To limit the influence of thermal errors during cutting, all the dimensional measurements are referred to a reference surface on the workpiece, obtained with repeated passes at the same nominal position, to remove the tool deflection effect. The effective deflection of each test is calculated as difference between the average profile coordinate of the test surface and the average profile of the reference surface.

A typical sample geometry is reported in Figure 5. It presents a stair-like geometry, one of the steps is always a reference surface, as described above, necessary to measure the deflection, while the other steps are the result of different machining conditions.

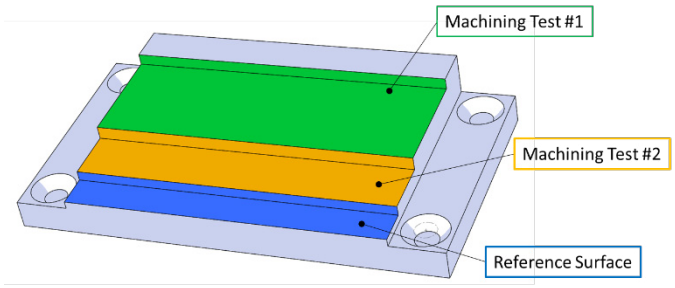

Fig. 5. Graphical representation of a workpiece after machining tests. Each sample has a reference surface (blue) and multiple machined surface, each for a single machining test (orange and green).

The positioning errors of the machine are measured locally using an indirect method. A reference sample with same geometry as the test samples has been completely machined with repeated passes, so as to remove the tool deflection contribution in all the generated surfaces. The dimensional measurement of such sample gives an estimation of the

positioning error during the specific cutting operation. Cutting forces were measured with a dynamometer, the Kistler 9139 model. The cutting tool used was an indexed cutter from Sandvik, R390-054Q22-17M, with TiAlN coated inserts. Inserts' geometry was measured with a focus variation profilometer, Alicona Infinite Focus, to characterize the cutting edge geometry.

3. Results

3.1. Stiffness characterization

In this section, the machine stiffness characterization results are presented. Figure 6 shows the force-displacement curve for the three different axis in all the positions tested. The X-axis and the C-axis present a distinct linear trend while for the Z-axis the behaviour appears to be close to a quadratic trend.

It is noted that the rigidity along the X-axis, the C-axis and partially also the Z-axis is affected by the position of the X-axis itself. In fact, the test positions C1 and C1.2 have a smaller X-coordinate (radial coordinate), changing the effective machine configuration (different overhang of the machine arm carrying the spindle) and consequently the overall stiffness. For the X-axis the effect becomes significant only for force values above approximately 1000 N. For the C-axis a change in the radial coordinate has a distinct impact on the circumferential stiffness at even low force values. The latter is decreasing from a stiffness of 1901 N/µm for the position C1.2, radial coordinate of 1347 mm, to a stiffness of 1278 N/µm, for a radial coordinate of 1569 mm, for the position C3.

Regarding the stiffness along the Z-axis, it can be noted that the rigidity is the highest as position C1.2, the one with the shorter radial coordinate. On top of that, the stiffness appears to decrease also moving from position C1 to position C4, that is moving from the top region to the bottom region of the hub. The latter behaviour is only present for the Z-axis stiffness and it is attributed to the geometry of the structure that holds the machine and connects it to the hub.

3.2. Offline compensation

Validation of the deflection model was carried out with side milling operation as previously described. Results of the lateral deflection, on the plane orthogonal to the Z-axis, are reported in Figure 7. A comparison between the model prediction and the measured deflection on the workpiece is shown. It can be noted that there is a good agreement between prediction and experimental values.

The model tends to overestimate the machine tool deflection for the test cases machined with radial immersion of 40 mm, however this overestimation is contained between 40 µm and 80 µm. The model discrepancy is related mostly to the an overestimation of the cutting force, inherited from the data-fitting approximations contained in the mechanistic cutting force model.

Tool-path compensation was validated with analogous side-milling tests. Figure8, shows a comparison between

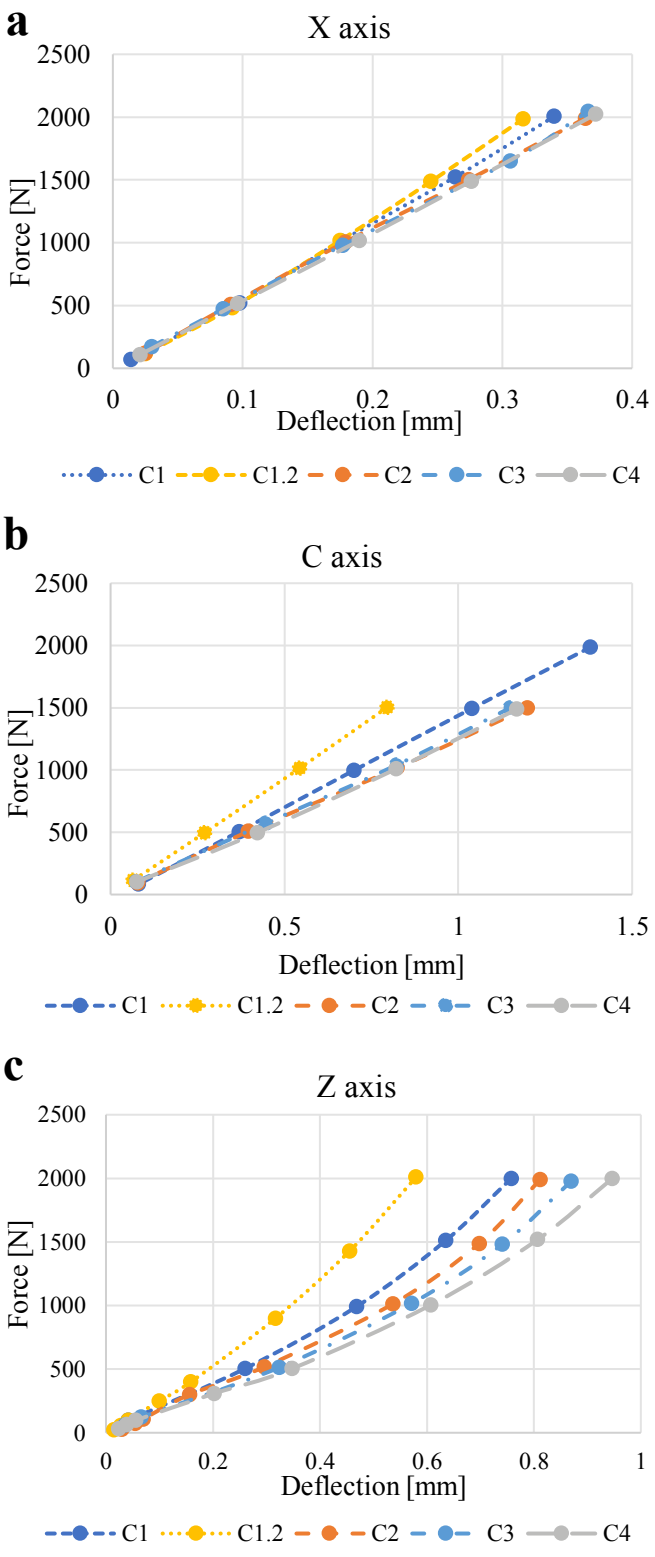

Fig. 6. Force-displacement data for each tested position C1-C4, relative respectively to the X-axis (a), the C-axis (b) and the Z-axis (c).

surface errors realized when the tool-path compensation is used or is not used with identical process parameters. The reduction in surface error is significant. As the deflection predicted by the model is slightly higher than the measured machine-tool deflection (red and blue bar) the tool trajectory modification realizes an overcompensation, from this derives the negative

values for the compensated tests. In all the three repetitions, a reduction of the cutting force induced errors of more than 88 % was achieved.

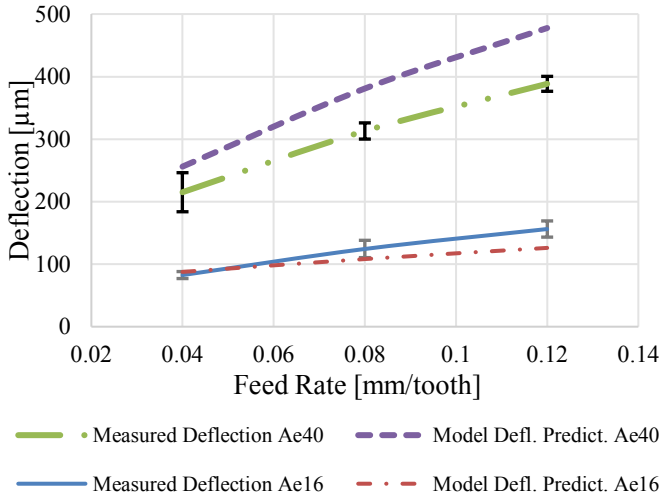

Fig. 7. Comparison between experimentally measured deflection and predicted deflection. Ap and cutting speed were kept constant at respectively 3 mm and 200 m/min.

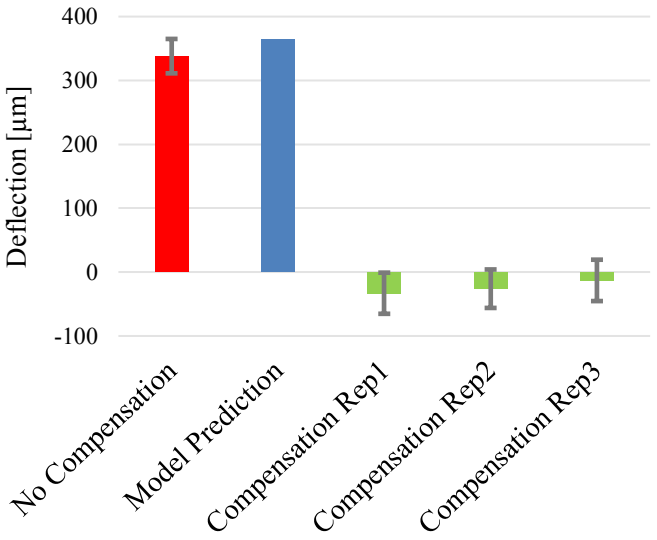

Fig. 8. Comparison between cutting force induced surface errors when compensation is activated or not activated. Negative values of surface error mean that the error is in the opposite direction in respect to the expected deflection

The standard deviation shown in Figure 7 and 8 are the result of the combined effect of the machine repeatability errors and the machine parallelism errors between the reference surface and the machined surface of each test related to the validation of the deflection model and the tool-path compensation. The expanded combined uncertainty associated with the deflection measurements in Figure 7 and 8 is 31 µm, calculated accordingly to [12]. In the calculation are considered the machine tool repeatability error, calculated to be 20 µm from the reference samples, the CMM maximum permissible error from certification and the form error on the part. A confidence of 95% was selected to calculate the coverage factor.

4. Conclusions

An offline compensation of the tool path for improved accuracy was implemented in a mobile, low-rigidity machine tool for application in the wind industry. The offline compensation was realized using a mechanistic cutting force model together with a characterization of the machine stiffness in the working volume. The deflection model was successfully validated through deflection measurements on linear path milling operations, hence the offline compensation was tested in similar milling operations. An improvement of accuracy of at least 88% was registered in the tested conditions.

5. Acknowledgements

The research studies presented in this article were carried out as part of the Innomill project, in part funded by the Innovation Fund Denmark. A special acknowledgement is expressed toward Finn and Aage from CNC-Onsite that helped greatly in the testing session.

6. Reference

[1] Blanco M. I. The economics of wind energy. Renewable and sustainable energy reviews 2009;13(6-7):1372-1382.

[2] Neugebauer R, Wabner M, Rentzsch H, Ihlenfeldt S. Structure principles of energy efficient machine tools. CIRP Journal of Manufacturing Science and Technology 2011;4(2):136-147.

[3] Lantz E, Wiser R, Hand M. The Past and Future Cost of Wind Energy; NREL/TP-6A20-53510. National Renewable Energy Laboratory, Golden, CO; 2012.

[4] Goch G, Knapp W, Härtig F. Precision engineering for wind energy systems. CIRP Annals-Manufacturing Technology 2012; 61(2):611-634.

[5] Uriarte L, et al. Machine tools for large parts. CIRP Annals-Manufacturing Technology 2013;62(2):731-750.

[6] Budak E., Altintas Y. Peripheral milling conditions for improved dimensional accuracy. Int. J. Mach. Tools Manufacturing 1994;34:907-918.

[7] Checchi A. et al. A mechanistic model for the prediction of cutting forces in the face-milling of ductile spheroidal cast iron components for wind industry application. Procedia CIRP 2018;77:231-234.

[8] W. A. Kline et al. The Prediction of Surface Accuracy in End Milling. Transactions of the ASME 1982;104(3):272-278.

[9] T. Seo, M. Cho, Tool Trajectory Generation Based on Tool Deflection Effects In Flat- End Milling Process (I). KSME International Journal 1999;13(10):738-751.

[10] Rao V. S., Rao P. V. M. Tool deflection compensation in peripheral milling of curved geometries. International Journal of Machine Tools & Manufacture 2006;46:2036-2043.

[11] Habibi M. et al., Tool deflection and geometrical error compensation by tool path modification. International Journal of Machine Tools and Manufacture 2011;51:439-449.

[12] JCGM100:2008 – GUM, Evaluation of measurement data – Guide to expression of uncertainty in measurement.